Geoderma 430 (2023) 116347

Contents lists available at ScienceDirect

Geoderma

journal homepage: www.elsevier.com/locate/geoderma

Heat-induced changes in soil water-extractable organic matter characterized using fluorescence and FTIR spectroscopies coupled with dimensionality reduction methods

M. Lado [a,*], J. Sayegh [b], A. Gia Gadñay [a], M. Ben-Hur [b], M. Borisover [b]

[a] AQUATERRA Research Group, Advanced Scientific Research Centre, University of A Coruña, CICA-UDC. As Carballeiras s/n, Campus de Elviña, La Coruña 15071, Spain
[b] The Volcani Institute, Soil, Water and Environmental Sciences, Agricultural Research Organization, Israel

ARTICLE INFO

Handling Editor: Cornelia Rumpel

Keywords:
Soil heating
EEMs
Mid-infrared spectra
PARAFAC
non-negative matrix factorization (NMF)

ABSTRACT

Water extractable organic matter (WEOM) is a very mobile and reactive soil OM fraction, critical in the translocation of carbon (C) from soils to other environmental compartments. Transformations of WEOM due to soil heating can have implications not only at a local scale, but in places far away from the location of the event. However, their accurate characterization is costly when analyzing a large number of samples. The objectives of this work were to identify common patterns for the changes in WEOM caused by the heating of various soil types using a combination of spectroscopic and dimensionality reduction techniques. Six soils from Spain, Kenya and Israel were collected at depths 0–10 cm and analysed before and after heating in air to temperatures of 300 and 600 °C. Fluorescence EEMs were measured in soil–water extracts containing WEOM, and decomposed using parallel factor (PARAFAC) analysis. The FTIR spectra were measured in freeze-dried extracts and further analysed using non-negative matrix factorization (NMF). Total organic C and $SUVA_{254}$ values of the extracts experienced changes with the heating treatments that were soil dependant. Four PARAFAC and three NMF components were sufficient to characterize WEOM changes in all soils, which showed common thermal transformation patterns irrespective of their origin and properties. Thermal transformation of fluorescent WEOM led to the increase in the proportion of a component with an emission maximum at Ex 300/Em 392 nm, and to a lower extent one with the emission maximum at Ex 300/Em 426 nm. Concomitantly, the proportion of components with emission maxima at longer excitation wavelengths was reduced. These changes occurred at the lowest heating temperature and were maintained at 600 °C, and they seem to indicate a depletion of fluorescent components more conjugated, bigger in size, and an enrichment in smaller ones. The NMF components obtained from FTIR spectra showed an increase of the proportion of compounds with C—O bonds, more oxidized. No correlations were found between the components obtained with each method, thus indicating that the information obtained from the fluorescence EEMs-PARAFAC analysis and the NMF decomposition of FTIR spectra is complementary. It can be concluded that there is a common pattern of WEOM changes induced by thermal soil transformations irrespective of the origin and properties of the soils studied, and that the combination of different spectroscopic techniques coupled with dimensionality reduction methods can be used as a simple and low-cost method to fingerprint changes in WEOM composition, in general, and those caused by soil heating, in particular.

1. Introduction

Wildfires are a disturbance that produce substantial changes in ecosystems, and they are perceived as one of the main global environmental threats (Doerr and Santin, 2016). The global annual area that has burned between 1997 and 2011 has been estimated to account for not<348 Mha (Giglio et al., 2013). Beyond the loss of aboveground living organisms, fire affects not only the location where it occurs. Pyrogenic materials can be exported from the fire-affected areas to water bodies even decades after the fire events occurred (Dittmar et al., 2012). Among the many effects of fires in ecosystems, soil physical, chemical and biological properties can be affected. These changes depend on the

* Corresponding author.

https://doi.org/10.1016/j.geoderma.2023.116347
Received 15 February 2022; Received in revised form 17 January 2023; Accepted 17 January 2023
Available online 24 January 2023

characteristics of the ecosystems and fire severity (Certini, 2005). Organic matter (OM) is one of the soil constituents most sensitive to heating: its transformations start at temperatures as low as 200 °C, and they comprise a series of complex reactions that depend on the temperature and the duration of heating (Knicker, 2007; Almendros and González-Vila, 2012; Miesel et al., 2015).

One of the most environmentally relevant fractions of soil OM is constituted by water-extractable compounds, which include soluble and colloidal particles grouped under the general term of water-extractable organic matter (WEOM), defined as the OM extracted by agitating soil samples with aqueous solutions (Chantigny, 2003). This is a highly heterogeneous pool of different molecular organic structures (Knicker, 2007), with varying molecular weight, functional groups, aromaticity, and hydrophilicity. Its content and composition are highly dependent on the soil type (Grandy and Neff, 2008), land use and vegetation (Roth et al., 2014), or climate (Kalbitz et al., 2000). The WEOM can interact with other soil constituents, like aluminium and iron (oxy)hydroxides (Vazquez-Ortega et al., 2014), or clay surfaces (Cheshire et al., 2008). As a very mobile and reactive soil OM fraction, it can form organo-metal complexes with heavy metals, modifying their mobility and bioavailability (Prokop et al., 2003), and it can also influence organic pollutant reactions in soils (Spark and Swift, 2002). It is ubiquitous, and it is the main vector for translocation of carbon (C) from the soil surface along the profile, and from soils to water bodies such as rivers, lakes and oceans. All the above-mentioned processes (i.e., pollutant movement, nutrient availability, formation of organo-metal complexes, contribution to aggregate stability and soil structure development, C sequestration) can be altered by changes in WEOM amount and composition as a result of soil heating (for example, during prescribed burning or wildfires). The heating/burning effects can have implications not only at a local scale, but in places far away from the location of the event. In the case of pyrogenic organic compounds, rivers are estimated to transport around 0.25 Pg C yr^{-1} from terrestrial to marine environments (Cauwet, 2002), and the current pool of thermally altered WEOM in the oceans is estimated to be 12 Pg C (Dittmar and Paeng, 2009).

Despite its obvious environmental importance, little is known about the changes in WEOM composition produced by fire and its fate. Studies focusing on changes in WEOM after fire are scarce, and they mostly examined changes in its content quantified in terms of organic C measured after filtering water extracts by 0.45 μm filters, which is commonly considered as the upper size limit of dissolved organic C (DOC). These studies reported decreases (Hobley et al., 2019) or increases (Alexis et al., 2010) in water-extracted DOC concentrations after fire. In addition, many of these studies focused on the solubility of black carbon compounds originating from charred litter (Revchuk and Suffet, 2014; Stirling et al., 2019; Jones et al., 2020), and not on the transformation of soil OM. Just a handful of references addressed changes in solubility and WEOM composition originating from the transformations of soil OM caused by fire. Vergnoux et al. (2011) analysed the effect of fire of different intensities and recurrence on WEOM characteristics in Mediterranean soils using ultraviolet–visible (UV–vis) and fluorescence spectroscopies, and suggested an increase in aromaticity of humified fractions for long time spans (more than 16 years) after the fire. Näthe et al. (2017) used solid state ^{13}C NMR to analyse changes in WEOM composition after a low intensity fire and found no differences immediately after the fire compared to an unburned control treatment, but an increase in aromaticity seventy days after the fire. Hobley et al. (2019) used a combination of UV–vis spectroscopy and machine learning algorithms to analyse the characteristics of WEOM in plots that were subjected to prescribed fire for more than 25 years, and observed a decrease in soluble C, as well as suggested an increase in its aromaticity. Most of these studies focused on DOC analysis, and ignored other C pools that are highly reactive and can contribute significantly to C translocation, like particulate and colloidal C (Yan et al., 2018), which have higher sizes than the one commonly assumed for DOC, and also different spectral properties (Näthe et al., 2017).

Current methods to characterize WEOM composition involve labour-intensive and costly techniques like nuclear magnetic resonance (NMR) spectroscopy, Fourier transform - ion cyclotron resonance mass spectrometry (FTICR MS), or pyrolysis–gas chromatography/mass spectrometry (Py-GC/MS), with limited applicability when the aim of the studies includes spatio-temporal characterizations that demand the analysis of a large number of samples. Thus, other spectroscopic techniques, faster and cheaper, are commonly applied, including UV–vis (Hobley et al., 2019), mid-infrared (Oren and Chefetz, 2012), or fluorescence (Ohno and BrO, 2006) spectroscopies. The essential limitation of these spectroscopic measurements, in highly heterogeneous mixtures, is that the obtained spectra are an integration of the various signals produced by different functional groups or types of molecules, which usually overlap. For spectroscopic analysis of these heterogeneous mixtures, it could be helpful to fractionate WEOM based on properties like size or electrophoretic mobility, but this results in a cumbersome task when the number of samples is large, and it does not ensure the integrity of the components during the separation process.

A convenient, faster and cheaper option to improve the spectroscopic analysis may be the mathematical transformation of a set of spectra in a sparse number of components that could explain the spectral variability in the dataset in terms of WEOM compositional changes. The most common mathematical procedures for this purpose include dimensionality reduction techniques like singular value decomposition (SVD; Henry and Hofrichter, 1992), independent component analysis (ICA; Wang et al., 2008) or principal component analysis (PCA; Ernakovich et al., 2015), which decompose the spectral signals in a limited number of components and provide also their relative contribution to each spectra. Looking to maximize statistical independence or to minimize correlation among components, these methods have the drawback of producing negative loadings, which do not correspond to the phenomenon under investigation, and thus their interpretation becomes difficult (Lee and Seung, 1999). An easier interpretation can be obtained ensuring that these analyses provide loadings with only positive values, which can be achieved introducing non-negativity constrains.

The use of parallel factor (PARAFAC) analysis for the decomposition of three-dimensional fluorescence excitation-emission matrices (EEMs) is an example of a very successful application of this approach (BrO, 1997; Ohno and BrO, 2006; Borisover et al., 2012). Due to the expected physical tri-linearity of excitation-emission phenomena, PARAFAC may provide, under certain conditions, unique decomposition of EEMs into contributions of chemically meaningful fluorescent components (BrO, 1997). Thus, the PARAFAC analysis has been used in studies covering different topics such as marine dissolved OM (DOM) composition and its sources (Murphy et al., 2008), lake and river seasonal dynamics (Borisover et al., 2009), speciation of organic compounds (Ritschel and Totsche, 2017), metal binding in sediments (Hu et al., 2019), or changes in DOM composition in drinking and wastewater treatment plants (Baghoth et al., 2011). Many studies have used PARAFAC for the analysis of dissolved fraction of WEOM in soils, where it has successfully identified the effects of manure applications (Sharma et al., 2017b) or irrigation water qualities (Borisover et al., 2012) on WEOM composition. It has been also used to analyse the dynamics of OM leaching in agricultural soils (Gu et al., 2019), and the differences in WEOM in soil profiles resulting from different land uses (Zhang et al., 2019). However, for bilinear datasets like those obtained by FTIR or UV–vis spectroscopies, the decomposition of spectra into a linear mixture of meaningful components becomes more complicated (de Juan and Tauler, 2021).

Since the publication of a seminal paper by Lee and Seung (1999), non-negative matrix factorization (NMF) has been extensibly recognized as an easily interpretable dimensionality reduction method for bilinear datasets, and it has been successfully applied in different fields including face recognition (Lee and Seung, 1999), text analysis, hyperspectral image analysis, imaging (Montcuquet et al., 2010; Sauwen et al., 2017), or genomics (Brunet et al., 2004; Yang and Seoighe, 2016). So far, its use to analyse WEOM spectral data is limited to a handful of studies

(Ritschel and Totsche, 2017; Fritzsche et al., 2019) despite its ability to provide unique solutions, besides scale and permutation variations, even when the signatures of different components overlap (Fu et al., 2018; Ang and Gillis, 2019; Fu et al., 2019).

We consider that analyzing compositional changes in WEOM originating from soils undergoing controlled heating in air could be useful to get a better understanding of a variety of complex processes taking place in soils during fire (e.g., Santos et al., 2016; Cawley et al., 2016; or Thurman et al., 2020). In this paper, we hypothesize that compositional changes in soil WEOM (containing DOC, colloidal and particulate OM, all chemically reactive and which can be mobilized by water) occurring as a result of soil heating can follow a common pattern irrespective of soil origin and properties. In addition, to our knowledge, the combination of fluorescence EEMs coupled with PARAFAC analysis and FTIR spectra decomposed using NMF have not been used yet to characterize the changes in WEOM caused by soil heating. Thus, the main objective was to characterize WEOM compositional changes in soils of different origin exposed to heating, using a combination of spectroscopic and dimensionality reduction techniques (PARAFAC for fluorescence EEMs, and NMF for FTIR spectra).

2. Materials and methods

2.1. Soil samples

Six soils were studied in this work (Table 1): three soils from Spain, two from Israel and one from Kenya. These soils were collected in order to cover different properties and origins in terms of climate (from semiarid to temperate humid), pH (from very strongly acidic to neutral), the presence of carbonates, and texture. These soils are representative of areas that are regularly affected by wildfires. At each site, samples were collected from the 0–10 cm mineral layer of non-cultivated plots, using a Dutch auger with a drilling diameter of 7 cm, after removal of the organic layer. Pooled samples were prepared at each site by mixing 5 sub-samples collected within a 4 m^2 area.

Samples were transferred to the laboratory, air-dried, and sieved to pass a 2-mm mesh. Characterization of the samples was conducted using standard methods: the texture was determined with a hydrometer (Gee and Or, 2002) after oxidation of OM with hydrogen peroxide; total organic C (TOC) content was measured using the Walkley-Black wet oxidation method (Nelson and Sommers, 1996); $CaCO_3$ content was determined by a volumetric method (Loeppert and Suarez, 1996); the cation exchange capacity (CEC) was measured by extraction with ammonium acetate at pH 7 (Sumner and Miller, 1996). The pH value and electrical conductivity (EC) were measured in 1:2.5 soil:water suspensions. All determinations were done in three replicates, and the above-mentioned soil characteristics are presented in Table 1. The soil texture ranged from sandy loam in the Spanish Rialta soil, to clayey in the Israeli Jerusalem and the Spanish Quinto soils. The TOC content ranged from 0.78 % in the Spanish semiarid Quinto soil to 5.17 % in the Israeli Mediterranean Jerusalem soil. In addition, two of the soils contained an amount of carbonates larger than 20 % in weight.

For each heating treatment, 5 g of a soil were placed in a ceramic crucible and exposed to the selected temperature in a muffle oven, open to the atmosphere. The purpose of this procedure was not to mimic the conditions under a wildfire or a prescribed one, but to ensure that all samples were exposed to the same heating treatment to test the hypothesis that WEOM transformations are similar irrespective of soil origin. In order to ensure that the soil properties, and especially TOC content and composition, were altered by the heating treatment and reached a stationary state, the soils were heated for 8 h. Two different heating temperatures were considered: 300 °C and 600 °C. Those represent temperatures that can be reached in moderate and intense fires, respectively. Around 300 °C, the most intense transformations of soil OM with heating occur (Knicker, 2007; McKay et al., 2020), while at 600 °C most of the OM is expected to be consumed (Certini, 2005). Although the 8 h heating at the indicated temperatures is not usual in wildfires, similar heating temperatures, sustained for long periods of time, can be found under smoldering conditions, when litter burns for hours (Rein et al., 2008). The heating experiments were conducted with three replicates for each soil and temperature.

2.2. Soil water extracts and characterization

The WEOM-containing extracts were obtained by mixing 3 g of unheated soil or soils obtained after the heating treatment with 20 mL of deionized water in a 50-mL centrifuge tube. The tubes were shaken at room temperature in an end-over-end shaker for 1 h and then centrifuged for 15 min at 2638 rcf in a HITACHI CR 22 N centrifuge (Tokyo, Japan). Following this process, the supernatant was filtered through a Whatman^{TM} 42 cellulose filter (2.5 μm pore size) and stored at 4 °C for further analysis, which were performed within a week from the extraction to ensure that no significant changes in the extracted WEOM occurred during storage (Rees and Parker, 2005; Rhymes et al., 2021). All WEOM extractions and further determinations were done in three replicates per soil/heating treatment for a total number of 54 samples, including controls, i.e., 6 soils × 3 treatments (2 heating temperatures plus an unheated control) × 3 replicates. Blank samples were prepared following the same steps to take into account possible artefacts and contaminations during the extraction process, which were not detected.

Table 1
Soil samples studied: location, type (IUSS Working Group WRB, 2015), climate, type of vegetation, particle size distribution, total organic C (TOC) and $CaCO_3$ contents, cation exchange capacity (CEC), and pH and electrical conductivity (EC) of the soil:water extracts. Numbers in parentheses indicate standard deviation.

Location	Country	Soil type	Climate	Vegetation	Particle size distribution			TOC	$CaCO_3$	CEC	Soil extracts (1:2.5)	
					Clay	Silt	Sand				pH	EC
					%, w/w					$cmol_c$/kg		dS/m
Mabegondo	Spain	Dystric Cambisol	Temperate	Shrubs	7.21 (0.42)	48.76 (1.13)	44.03 (1.48)	1.8 (0.03)	0.4 (0)	10.91 (0.09)	5.03 (0.04)	0.09 (0)
Rialta	Spain	Dystric Cambisol	Temperate	Coniferous trees, shrubs	5.11 (0)	24.68 (0.85)	70.21 (0.85)	4.53 (0)	0.4 (0.03)	13.02 (0.18)	4.95 (0.02)	0.16 (0)
Quinto	Spain	Haplic Calcisol	Semiarid	Shrubs, anual plants	57.60 (0.03)	34.00 (0.01)	8.40 (0.02)	0.78 (0.01)	21.6 (0.03)	17.97 (0.85)	7.2 (0.05)	0.66 (0.01)
Ngata	Kenya	Umbric Andosol	Temperate	Scattered trees, shrubs, anual plants	7.82 (0)	44.36 (0)	47.82 (0.01)	4.82 (0)	0 (0)	22.46 (0.73)	5.95 (0.08)	0.44 (0)
Menashe hills	Israel	Rendzic Leptosol	Mediterranean	Shrubs, anual plants	15.50 (0.75)	34.46 (1.83)	50.04 (1.45)	4.46 (0.04)	59.9 (0.61)	19.89 (0.24)	7.24 (0.05)	0.27 (0.01)
Jerusalem mountains	Israel	Chromic Luvisol	Mediterranean	Coniferous trees, shrubs	47.77 (0.45)	22.53 (0.45)	29.70 (0.01)	5.17 (0.01)	1.7 (0.06)	37.52 (0.68)	7.08 (0.04)	0.17 (0.02)

The UV–vis absorbance of the filtered soil extracts was measured in a 1-cm quartz cuvette in the 200–1000 nm range in 2 nm increments using a Zuzi UV–vis 4418 spectrophotometer (Auxilab, Spain). When the absorbance of the samples was above 1.5, extracts were diluted to ensure that the measurements were done in the range of concentrations where Lambert-Beer law applies (Kothawala et al., 2013). Organic C of the water extracts was measured in a Shimadzu 5000A TOC Analyser (Kyoto, Japan) after acidification of the samples to remove carbonates. The specific UV absorbance at 254 nm ($SUVA_{254}$ index), commonly used to characterized WEOM, was calculated as the ratio of absorbance at 254 nm and TOC measured in the extracts, divided by the optical path (1 cm) and multiplied by 100.

2.3. Fluorescence measurements of soil extracts

Fluorescence EEMs were measured in the extracts or their dilutions using a Horiba FluoroMax® – 4P spectrofluorometer (Kyoto, Japan). Excitation wavelengths were between 220 and 520 nm, and emission was measured at wavelengths between 224 and 700 nm, both in 4 nm increments and slits of 4 nm. The minimum excitation wavelength was chosen to ensure that absorbance of the samples was below 1.5 absorbance units, which is the upper limit for effective inner filter effect corrections based on absorbance values in 1-cm cells (Kothawala et al., 2013). For each excitation wavelength, emission intensities (S) were corrected against those measured in a reference detector (R) as the ratio S/R, to account for differences in the intensity of the excitation light. The obtained EEMs were corrected following several steps:

- The intensity of fluorescence emission in all regions with excitation wavelengths larger than the emission wavelengths was considered to be 0.
- Intensities of fluorescence emission in regions corresponding to 1st, 2nd and 3rd order Rayleigh scattering were considered as missing values.
- Inner filter effect of the samples, caused by the absorption of exciting light and reabsorption of the emitted light, was corrected using the data on UV–vis absorbance previously measured in the spectrophotometer, following the equation (1) (Lakowicz, 2013):

$$F_c = F_m \times 10^{((Abs_{ex}+Abs_{em})/2)} \quad (1)$$

where, F_c is the corrected fluorescence intensity; F_m is the measured fluorescence intensity; Abs_{ex} is the absorbance of the sample measured at the excitation wavelength, and; Abs_{em} is the absorbance of the sample measured at the emission wavelength.

- In order to remove interferences with water Raman light scattering, the corresponding EEMs of blank samples (corrected also following the previous steps) were subtracted from those of soil–water extracts.
- Any remaining negative fluorescence values were considered as missing values.

The resulting EEMs were expressed in Raman units using water Raman peak intensity at ex/em 300/397 nm (Holbrook et al., 2006) and subjected to PARAFAC analysis to identify the individual components that could explain the variability of EEMs across the whole dataset of soil extracts. Total fluorescence of each EEM was calculated as the sum of all emission intensities in the EEMs reconstructed using the components and scores obtained from PARAFAC. The use of reconstructed EEMs instead of the original ones for this calculation was caused by the fact that the latter ones contain missing values in those areas where the effect of Rayleigh scattering was removed, while this is avoided in the reconstructed EEMs due to the missing value imputation capabilities of PARAFAC.

2.4. Fourier transform infrared spectra measurements of water-extracted soil material

The FTIR spectra of soil–water extracts were measured in transmission mode, using KBr pellets, as follows: A 1-mL aliquot of the soil–water extracts was mixed with 200 mg of potassium bromide (KBr - FTIR grade-Panreac) and immediately frozen to −60 °C. The frozen mixture was freeze-dried for 24 hrs in a Telstar Cryodos-80 lyophilizer (Barcelona, Spain), ground to a fine homogenized powder in an agate mortar under an IR lamp to reduce absorption of air humidity by the mixture, and then pressed to 2 MPa using a Specac Mini Pellet Press to produce a KBr pellet. The mid-IR spectra of the pellets were measured in a Thermo Scientific is10 FTIR spectrometer (Madison, USA), in transmission mode, at wavenumbers between 630 and 4000 cm^{-1} with a resolution of 2 cm^{-1}. Each sample was scanned 128 times, and the final IR spectrum was the average of these spectra. After collection, a Savitzky-Golay filter was applied in order to remove noise, and baseline and scatter effects were corrected using a Extended Multiplicative Scatter Correction (EMSC) method (Afseth and Kohler, 2012), using the package EMSC (Liland, 2021). Then, the spectra were subjected to a non-negative matrix factorization (NMF) using an Anchor free method (Fu et al., 2019).

2.5. Spectral decomposition and statistics

All spectral corrections, calculations and statistical analysis were conducted with R-Studio (R Core Team, 2021). The PARAFAC analysis of three-dimensional EEMs was implemented using the R package multiway (Helwig, 2019). The NMF analysis of bilinear FTIR spectra was performed using the R package vrnmf (Soldatov et al., 2021). In both decomposition methods, PARAFAC and NMF, the rank or number of components that explain the variability of the samples is the most important parameter that needs to be chosen. Rank selection was done using an approach based on crossvalidation, taking advantage of the capability of both methods for missing data imputation, in a hold-out strategy as follows (BrO, et al., 2008): the spectrum of one of the three replicates for each soil and heating treatment (and control) was randomly selected and set aside to form a held-out or test set. The remaining spectra, or training set, were used to fit the models with different number of components from 2 to 10. Each EEM or FTIR spectrum in the held-out set was divided randomly in 5 folds or groups of data. The components obtained in each fitting procedure performed on the training set were used to fit the spectra to four of the folds in the held-out group, and to predict the values corresponding to the fifth fold. The procedure was repeated for each fold, so all data in the held-out spectra was used for fitting and validation. Errors were calculated as the difference between the predicted values and the measured ones. Coefficients of determination R^2 of the regression of predicted vs observed values, and Predicted Errors Sum of Squares (PRESS) were used to identify the proper number of components. The procedure was repeated 30 times, each time with different random folds divisions. Final R^2 and PRESS values were computed as the average of their values obtained for each EEM or FTIR spectrum and each of the 30 iterations. Model rank was selected as the one that provided minimum and maximum values of PRESS and R^2, respectively. In the case when these parameters showed a constant improvement with increasing number of components, the selected rank was the one from which any further addition of new components resulted in small PRESS and R^2 variations.

Average values of component scores were calculated for each soil and heating treatment, and one-way ANOVAs were performed in order to test for significant differences in means caused by the heating treatments in each soil. In those cases where significant differences were found, post-hoc Tukey's Significant Differences tests (Steel and Torrie, 1960) were conducted to identify differences between treatments. All statistical tests were performed at the $P < 0.05$ significance level.

3. Results

3.1. Heating effect on TOC content and $SUVA_{254}$ determined in soil extracts

Table 2 shows TOC amounts extracted from the soil samples and referred to soil mass and to the TOC content in the soils. Heating the soils at 300 °C did not produce any significant change in the amount of TOC per soil mass except in the Rialta soil, where it decreased by 90 %, and the Quinto soil, where it increased by 206 %. A further increase of the heating temperature to 600 °C resulted in significant decreases of TOC amounts referred to soil mass except in Mabegondo and Rialta soils, where this reduction was not significant compared to the value obtained at 300 °C (although in all soils, the reduction was significant compared to the unheated samples).

When analysing the amount of TOC in the extracts relative to TOC content in the soils, it can be observed that heating at 300 °C increased the percentage of OC that is water-extractable, although this increase was not significant in the case of the Jerusalem soil. Exception to this observation is the Rialta soil, where heating decreased the contribution of TOC in the extracts to soil TOC content by 80 %. At 600 °C, TOC contribution also increased significantly compared to the unheated one, except in Quinto and Rialta, where it decreased although not significantly. Similar soil-dependant behaviour was observed for $SUVA_{254}$ (Fig. 1). Heating the soils at 300 °C increased its value in four out of the six analysed soils, while when the temperature used was 600 °C, $SUVA_{254}$ decreased to values lower than those observed in the non-heated soils (with the exception of Quinto soil, where the values were similar).

4. Heating effect on fluorescence of soil extracts

4.1. Total fluorescence

Table 3 provides the data on the total fluorescence of the soil extracts and the values of specific fluorescence emission, obtained as a ratio between total fluorescence emission and TOC concentration in extracts. The former reflects the presence of fluorescent OM in water extracts whereas the latter is related to the fraction of the fluorescent OM in the whole WEOM pool. The total fluorescence increased in the samples obtained after heating soils at 300 °C, as compared with non-heated samples, except the Rialta and Mabegondo soils, where differences were not statistically significant. A further increase of the heating temperature to 600 °C led to the decrease of fluorescence compared to the values obtained at 300 °C in all cases except the Rialta soil. The specific fluorescence emission increased when the soil was heated to 300 °C compared to the unheated soil (Table 3). However, heating to 600 °C resulted in fluorescence values intermediate between those of the other treatments with the exception of Mabegondo soil, where fluorescence after heating at 600 °C was the smallest, and Ngata, where it was the highest.

4.2. PARAFAC-identified fluorescent components presented in soil extracts

Based on the R^2 and PRESS values obtained through crossvalidation, the optimal number of components in the PARAFAC model was 4, with a PRESS of 5,536 and a R^2 of predicted vs observed values of 0.998. The EEMs and excitation and emission spectra of the four components are presented in Fig. 2: component 1 has a maximum at Ex 300/Em 392 nm; component 2 shows a maximum at Ex 300/Em 426, with a secondary excitation maximum at 236 nm; component 3 shows a fluorescence maximum at 236/420 nm; finally, component 4 is characterized by a maximum at Ex 256/Em 488, with a secondary excitation maximum at 368 nm.

Some of these components have been found in PARAFAC analysis of WEOM from different origins. For example, component 1 has been found previously in Mediterranean soils, and it was considered small in size, with limited biodegradability, and low ability to adsorb to soils and sediments (Ishii and Boyer, 2012; Sharma et al., 2017a). Component 2 has been observed in soils too, where its contribution to fluorescence decreased during decomposition of biomass (Hunt and Ohno, 2007). It has been considered similar to a microbial-derived humic peak designated as M, composed of relatively aliphatic compounds with low molecular weight (Lambert et al., 2016; Podgorski et al., 2018). Component 3 has been also ascribed to microbial degraded humic-like substances. Its excitation and emission spectra resemble those of oxidized quinones (Cory and McKnight, 2005) and it has been found to correlate with lignin content in soil and water samples (Fellman et al., 2009). It has been described as formed by compounds with low molecular weight, high aromaticity, and high O/C ratio, indicating a high degree of oxidation (Podgorski et al., 2018). Finally, component 4 has been found previously in many environments like forest and agricultural streams, seawater or soils (Baghoth et al., 2011; Ishii and Boyer, 2012; Sharma et al., 2017a). It has been characterized as being a humic-like fluorescent component from terrestrial origin, and due to the longer excitation and emission wavelengths compared to the other components, it has been suggested that it is larger in size, more condensed and conjugated than the other three. It has been described as biodegradable, plant-derived OM produced by microbial transformations (Hunt and Ohno, 2007; Sharma et al., 2017a). Some others have described this component as consisting of molecules with large molecular size and hydrophobic characteristics (Ishii and Boyer, 2012), and it has been related to the presence of reduced quinone-like components of WEOM (Cory and McKnight, 2005).

In order to examine the compositional changes in fluorescent WEOM caused by soil heating, ratios between the PARAFAC scores of the four components were calculated, and are presented in Fig. 3. Heating

Table 2
Total organic C (TOC) determined in soil extracts and referred to the soil mass, and its percentage referred to TOC in the soil for all the studied soils after the different heating treatments.

Heating temperature, °C	Soil samples					
	Mabegondo	Rialta	Quinto	Ngata	Menashe	Jerusalem
	TOC, mg g $soil^{-1}$					
NH[a]	0.26 a*	1.05 a	0.27b	0.75 a	1.07 a	1.03 a
300	0.17 ab	0.10b	0.81 a	0.83 a	1.03 a	1.03 a
600	0.08b	0.06b	0.08c	0.10b	0.14b	0.12b
	$TOC_{extracts}/TOC_{soil}$, %					
NH[a]	1.16b	2.32 a	3.43b	1.55c	2.39b	2.00b
300	3.86 a	0.47b	15.70 a	5.31b	5.65 a	2.90b
600	4.36 a	2.23 a	1.99b	9.27 a	5.26 a	26.72 a

[a] NH – Not heated; * Different letters indicate significant differences between heating treatments for each soil ($P < 0.05$).

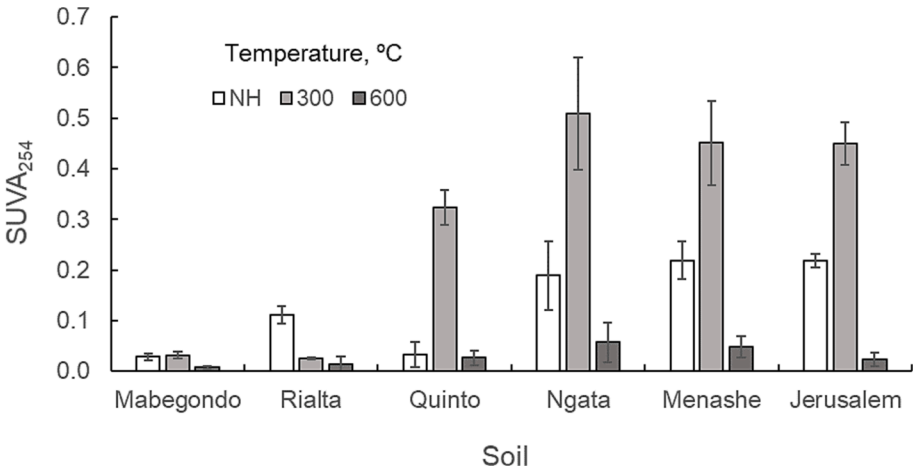

Fig. 1. $SUVA_{254}$ values for all soils and heating treatments. Bars represent standard deviation. NH: Not heated.

Table 3
Total fluorescence in Raman units (R.U.) and specific fluorescence emission (ratio between total fluorescence in R.U. and TOC in mg L^{-1}) in the soil extracts for all the studied soils after the different heating treatments.

	Soil samples					
Heating temperature, °C	Mabegondo	Rialta	Quinto	Ngata	Menashe	Jerusalem
	Total fluorescence, R.U.					
NH[a]	104,964 a*	155,247 a	50,908b	180,978b	263,496b	215,757b
300	161,207 a	122,559 a	1,200,036 a	2,650,541 a	2,142,323 a	1,818,666 a
600	11,470b	59,716 a	78,208b	343,883b	198,558b	114,041b
	Total Fluorescence/$TOC_{extracts}$, R.U. L mg^{-1}					
NH[a]	352b	136b	192b	214c	222b	189b
300	888 a	1,080 a	1,300 a	2,785b	1,885 a	1,575 a
600	126c	415 ab	830 ab	4,359 a	1,292 ab	727 ab

[a] NH – Not heated; * Different letters indicate significant differences between heating treatments for each soil ($P < 0.05$).

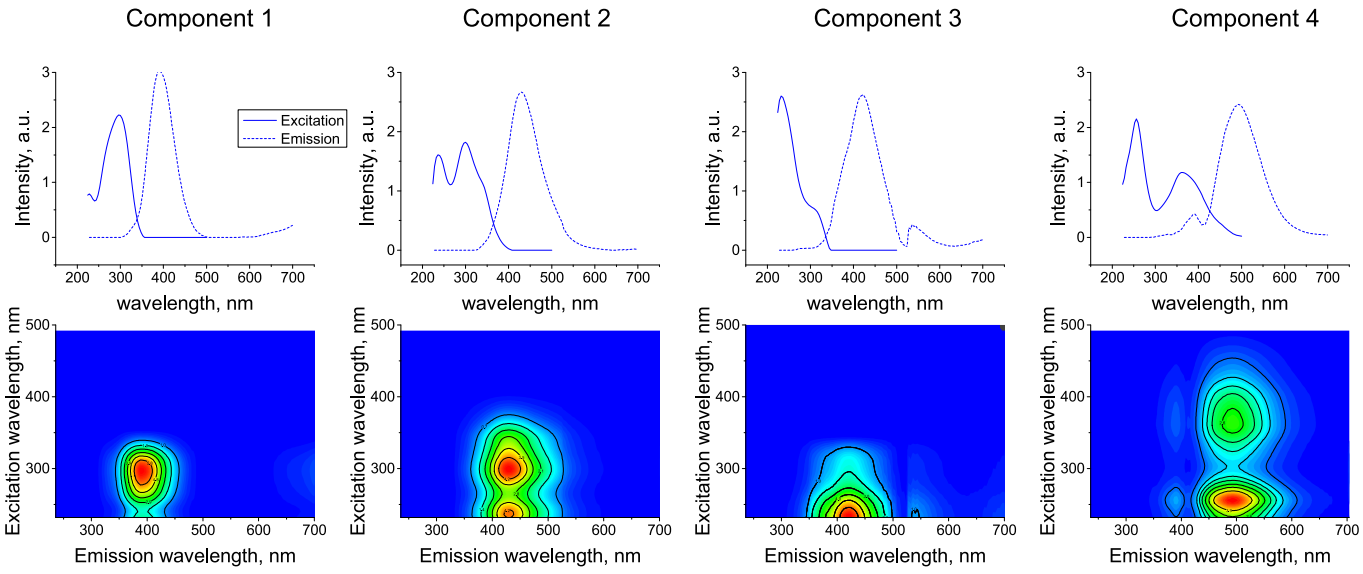

Fig. 2. EEMs and excitation and emission spectra of the four components detected in aqueous soil extracts using PARAFAC analysis.

produced significant changes in the ratios of the PARAFAC components scores, and some trends were consistent in all soils. The ratios between the scores of component 1 and the ones of the other three components (Fig. 3a, b and c) increased in all soils when heated. This increase was observed at the lowest heating temperature (300 °C), suggesting an increase of the contribution of this component to the fluorescence EEMs of extracts when heating the soils. Rising the heating temperature to 600 °C did not produce a further increase of the ratios where this component is involved. A similar behaviour was observed for the ratio of the PARAFAC scores between components 2 and 4 (Fig. 3e). The scores

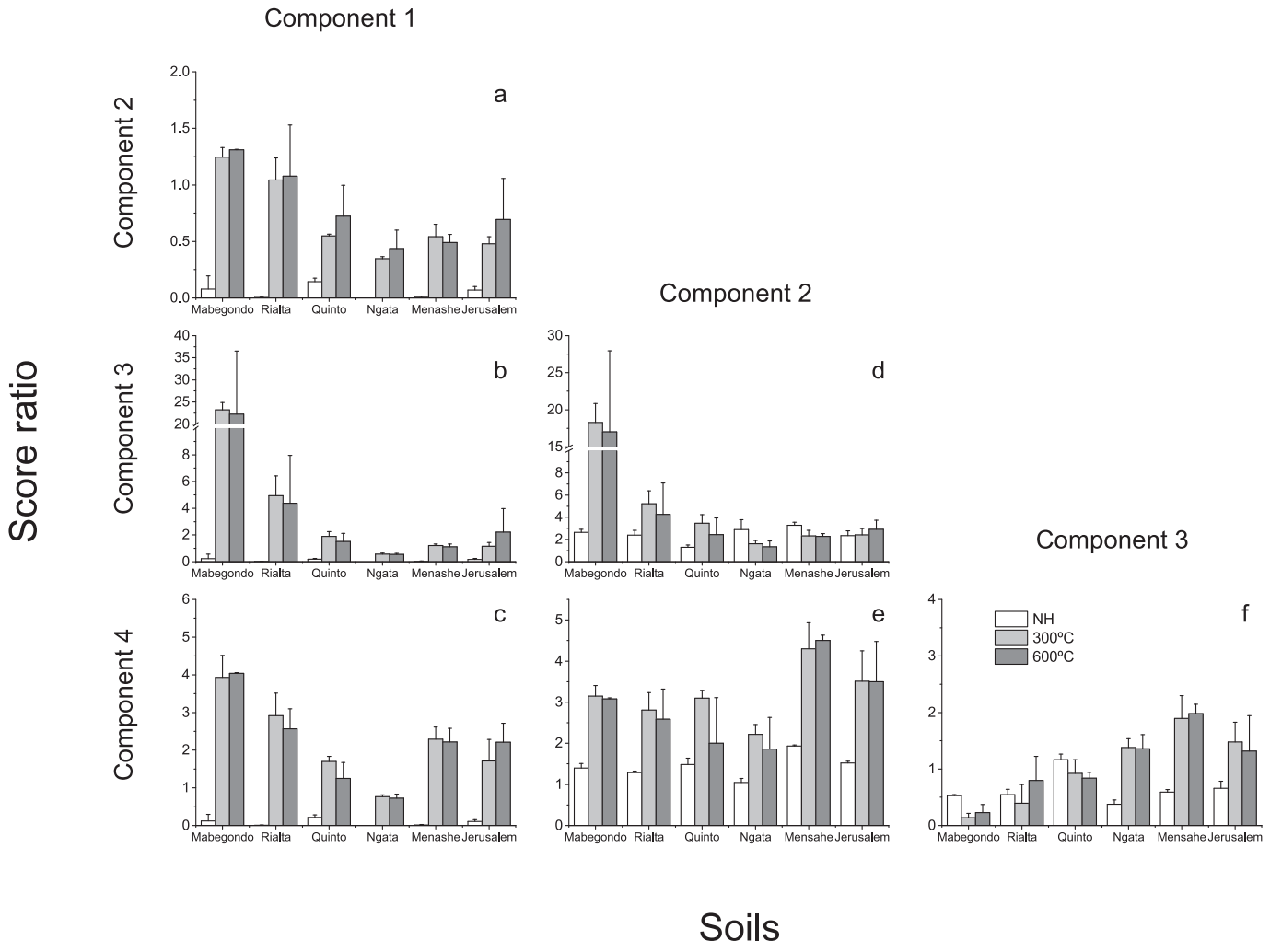

Fig. 3. Ratios of the scores for the four components obtained with PARAFAC on WEOM fluorescence EEMs, for all soils and heating treatments. The first (left) column of the plots provides the ratios between the scores of component 1 and the scores of components 2 (a), 3 (b) and 4 (c). The second (middle) column of the plots reports the ratios between the scores of component 2 and the scores of components 3 (d) and 4 (e). The right plot shows the ratios between the scores of components 3 and 4 (f). Bars indicate standard deviation. NH: Not heated.

ratio between component 2 and component 3 (Fig. 3d) shows a more soil-dependant behaviour, with an increase when the soil was heated to 300 °C in some soils (Mabegondo, Quinto and Rialta), while in other cases this ratio does not change with heating (Menashe and Jerusalem) or even decreases (Ngata). Finally, the behavior of score ratios between components 3 and 4 (Fig. 3f) was also not consistent for all soils and temperatures, with some soils like Ngata, Menashe and Jerusalem showing increases in this ratio when heated, while the others showed no change in the score (Rialta and Quinto) or even a decrease (Mabegondo).

4.3. Heating effect on FTIR spectra of soil extracts

Identification of the components controlling FTIR spectra of WEOM was done following the crossvalidation procedure described in the material and methods section. The optimal number of components of the fitted NMF model was 3, with a PRESS value of 16.3 and R^2 of predicted vs observed values of 0.999. The loadings of the three NMF components are presented in Fig. 4. Since NMF decomposes the input matrix in an additive mixture of those non-negative components, each component is considered to be chemically meaningful and characterized by a variety of IR-active functional groups. Component 1 is characterized by a maximal absorbance at 655 cm^{-1}, found to be O—H out of plane vibrations of carbohydrates (Abdulla et al., 2010). A very strong absorption includes a narrow band with the peak at 1100 cm^{-1} (C—H deformation of unsaturated hydrocarbons; Li et al., 2015). Absorbance at 1128 cm^{-1} reflects C—O strectching of aliphatic OH (Li et al., 2015), and that at 1192 cm^{-1} reflects C—O stretching vibrations of aryl ethers and phenols (Parikh et al., 2014; Silverstein et al., 2015; Li et al., 2015). In addition, there is a broad absorption band with a series of small peaks, identified at 1426 and 1478 cm^{-1}, which correspond to the area of C=C stretches (Oren and Chefetz, 2012), although the one at 1426 cm^{-1} has been also reported as produced by carboxyl groups in humic acids (Artz et al., 2008). The peak at 1622 cm^{-1} is related to both carboxyl groups and aromatic structures, but the contribution of carboxyl groups dominates, as shown by the shoulder at 1686 cm^{-1} (Oren and Chefetz, 2012).

Component 2 shows a peak at 800 cm^{-1}, usually identified as aromatic C—H out of plane vibrations (Niemeyer et al., 1992) and NH_2 of primary amides; a broad peak at 1026 cm^{-1}, which corresponds to the region of C—O stretching and bending commonly associated with polysaccharides and polysaccharide-like compounds, including cellulose and lignin (Parikh et al., 2014; Traoré et al., 2016; Matamala et al., 2017). Small peaks at 1176 and 1232 cm^{-1} are sometimes included in the range of C—O aliphatic vibrations (Kalakodio et al., 2017) but in other cases assigned to aromatic C—H vibrations (Ilani et al., 2005) or phenolic C—O—C stretches (Parikh et al., 2014). A sharp peak at 1380 cm^{-1} could be due to C—H bending of polysaccharides and aliphatic

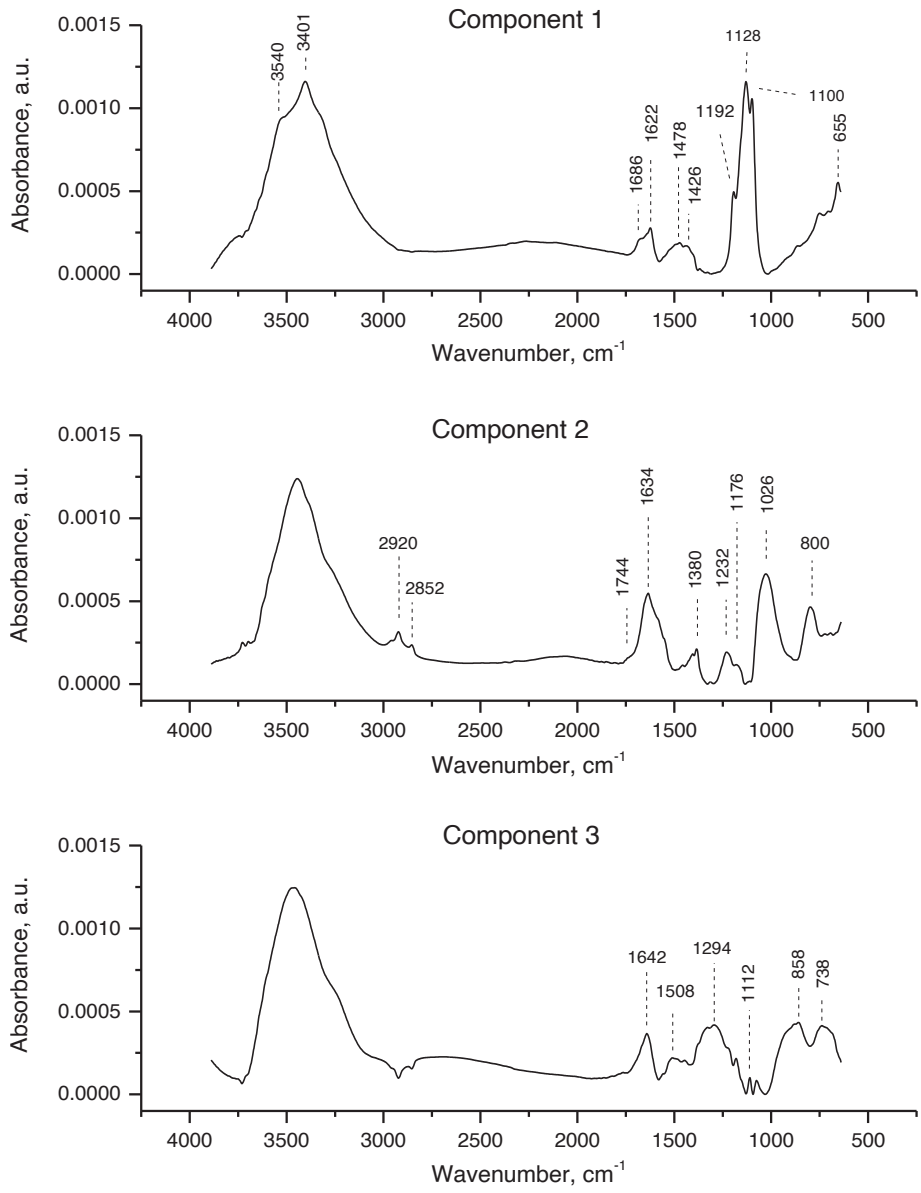

Fig. 4. Spectra of the three components extracted using NMF for the decomposition of FTIR spectra.

compounds (Oren and Chefetz, 2012), but in combination with the peak at 1634 cm^{-1} it could be indicative of carboxylic stretching (Guo and Chorover, 2003). This last peak, together with the shoulder at 1550 cm^{-1}, is also indicative of aromatic C═C vibrations (Kaiser et al., 1997; Oren and Chefetz, 2012). The peak at 1744 cm^{-1} indicates the presence of undissociated forms of carboxyls (Gu et al., 1995; Parikh et al., 2014) and carbonyls (Matamala et al., 2017). Finally, bands at 2852 and 2920 cm^{-1} are produced by aliphatic CH groups.

Component 3 has major peaks at 738, 858, and 1112 cm^{-1}, resulting from aromatic out of plane C—H vibrations (Ilani et al., 2005; Peltre et al., 2014; Parikh et al., 2014). The peak at 1294 cm^{-1} is commonly attributed to in plane C—OH an C—H vibrations of phenols and aromatics (Peltre et al., 2014). The peak at 1508 cm^{-1} is typical for aromatic C═C vibrations (Matamala et al., 2017). The absorbance at 1642 cm^{-1} corresponds to C═O vibrations (Parikh et al., 2014).

Compositional changes in WEOM induced by different thermal treatments of the soils are expressed in Fig. 5 as the ratios of NMF scores between the different pairs of components, i.e., 1 and 2, 1 and 3, and 2 and 3. Heating produced changes in these ratios, although their dynamics seem different than those observed for the $SUVA_{254}$ and the PARAFAC components: for FTIR spectra, the most important changes were produced at a heating temperature of 600 °C, where the score ratios of component 1 with the other two increase in most soils, although sometimes this increase was not significant. However, the scores ratio between components 2 and 3 did not show a consistent behaviour. In general, it did not change with temperature, except in Ngata, where it increased at a temperature of 600 °C, and Menashe, where the increase occurred at 300 °C.

5. Discussion

5.1. Heating effect on OM solubility, specific UV absorbance and bulk fluorescence

Soil heating in the presence of air led to changes in WEOM amount expressed as TOC per mass unit of soil in most soils, probably linked to the oxidation and mineralization of soil organic C (Knicker, 2007). Also, the organic C in the heated soils was constituted by more extractable compounds, as observed from TOC amounts in the extracts referred to soil TOC. However, the temperature at which these two processes led to

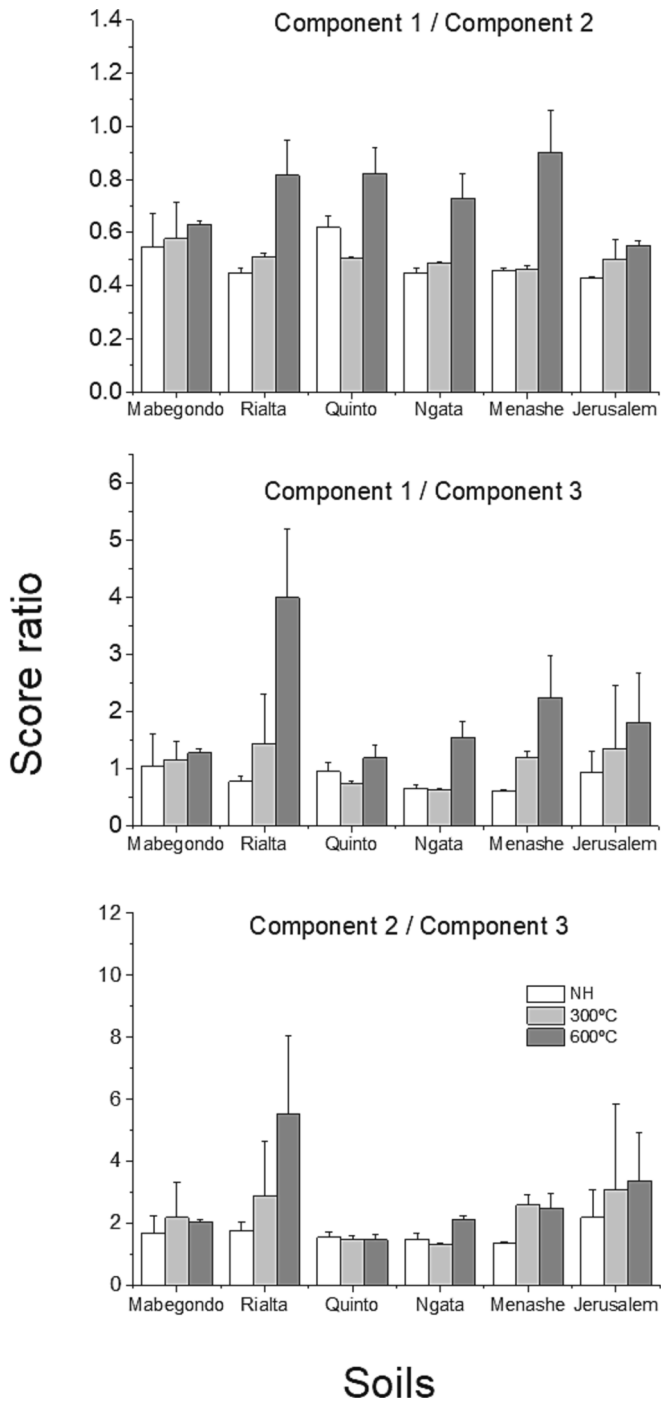

Fig. 5. Ratio of the NMF scores extracted from FTIR WEOM spectra between different pairs of the components, i.e., 1 and 2, 1 and 3, and 2 and 3, for all soils and heating treatments. Bars indicate standard deviation. NH: Not heated.

significant changes in these parameters was not the same in all soils, and thus the results were not consistent. Previous studies observed an increase in the amount of soluble organic C when soils where heated (e.g., Cawley et al., 2016; Thurman et al., 2020), reaching a maximum at 225 °C and a progressive decline with a further increase of the heating temperature, until it became undetectable at 500 °C. Cawley et al. (2016) observed that TOC values in water extracts after heating the soil at 350 °C could be higher or lower than those of unheated soils, depending on the rate at which TOC amounts decrease from the maximum value obtained at 225 °C with the exposure to temperatures increasingly higher than this value. These differences could be related to the nature of the existing OM or to other soil properties like texture and clay mineralogy, which could protect soil OM from thermal decomposition. However, it is clear that heating at 300 °C resulted in a more water-extractable bulk composition of the remaining OM except in Rialta soil. Oxidation of soil OM in the presence of air at this temperature may lead to the formation of hydrophilic substances, most probably characterized also by smaller size/molecular masses than those found in unheated soils (Cawley et al., 2016; Thurman et al., 2020). Smaller molecular weights and increased hydrophilicity should enhance aqueous solubility/extractability of organic components present in soils.

Changes in soil OM extractability were accompanied by changes in WEOM composition, as infered by changes in the optical properties of the extracts. Heating soils at 300 °C increased $SUVA_{254}$ in four of the soils. This parameter is commonly related to the presence of aromatic compounds in WEOM (Weishaar et al., 2003), and thus it should be assumed that OM transformations resulted in a larger proportion of aromatic compounds in the WEOM of some of the soils. Similar results were found by other studies, relating changes in WEOM at a temperature around 300 °C with a decrease in molecular weight and a general increase in aromaticity inferred by $SUVA_{254}$ (McKay et al., 2020); however, similar to the present study, this trend seems to be soil-specific and sometimes not consistent with the determinations of aromatic C by NMR (Santos et al., 2016), suggesting that this parameter might not be the most adequate to characterize OM aromaticity in soil–water extracts of heated soils.

Heating at the highest temperature apparently reduced the proportion of aromatic compounds in WEOM, as compared with both the non-treated soils and those heated at 300 °C. Since heating at 600 °C decreased TOC concentrations in soil extracts as compared with the other treatments, the decline in $SUVA_{254}$ suggests that concentrations of hydrophilic water-soluble aromatic compounds decreased to a higher degree than aliphatic water-soluble compounds. One explanation for this behaviour could be that high temperatures, besides more intense oxidation of OM, induce condensation/polymerization reactions of soil OM materials (e.g., humic substances or their residuals) leading to the accumulation of humin-like organic components in the soil (Fernández et al., 1997; González-Pérez et al., 2004). Such polymerized larger-size aromatic compounds resist extraction by water, thus leading to water extracts showing lower humic fractions and higher proportions of aliphatic compounds. Formation of charred OM at this temperature might also reduce the fraction of water-soluble aromatic compounds (Trompowsky et al., 2005; Knicker, 2007), thus contributing to more aliphatic WEOM.

Total fluorescence data revealed that heating at 300 °C produced soil extracts enriched in fluorescent (and most probably, aromatic) material except in the Rialta soil. Heating at 600 °C reverted the trend, leading to the reduction of fluorescent material as compared with the soils heated at 300 °C. It appears that the release of water-extractable fluorescent OM, predominantly composed of humic substances as inferred from the extracted PARAFAC components, was stimulated by heating at this temperature. Oxidation of soil OM and its thermal degradation in air resulted in the formation of water-soluble aromatics (González-Pérez et al., 2004; Knicker, 2007); higher temperature may convert them into charred, condensed or polymerized material, preventing physically or chemically its dissolution into the aqueous medium (Knicker, 2007; Mitchell et al., 2015). Altogether, WEOM becomes enriched in fluorescent material after heating at 300 °C as seen from the TOC-normalized fluorescence, but a higher temperature produces a general reduction of the contribution of fluorescent OM to TOC except in one soil. Different dynamics in composition of WEOM, depending on the temperature of heating, are of interest: consideration of aromatic vs aliphatic nature of WEOM may be helpful to understand whether WEOM, produced or modified after soil heating/burning, will effectively interact with minerals, how it will move in the soil profile, and what its impact on interactions with chemicals in soil solutions is. For example, the presence of significant aromatic fraction in WEOM might be seen as an important

contributor to binding interactions with aromatic pesticides, pharmaceuticals or PAHs and affect their environmental fate (Sun et al., 2013). Also, resistance to microbial degradation is expected to be affected by aromatic vs aliphatic nature of WEOM (Hadas et al., 2004).

5.2. Thermal transformations and spectral decomposition

Contrary to the variable behaviour of OM solubility, UV indices and total fluorescence with temperature, a good indicator of the presence of transformed WEOM with soil heating is the change in the proportions between concentrations of different components identified from the spectral signatures. Regarding the PARAFAC-identified fluorescent components, the most noticeable change when the soils were heated was the increase in the concentration of component 1 compared to the concentrations of the other three components. This is evident in the score ratios, since the score ratios are proportional to the concentration ratios, and therefore, their dynamics may be quantitatively monitored in a series of samples. Similarly, an increase in the scores ratio of components 2 and 4 was observed in all soils. An increase in blue-shifted PARAFAC components in WEOM from soils heated at temperatures of 350 °C was also found by Cawley et al. (2016). It could be assumed that, the longer the emission wavelength, the higher the molecular weight of a fluorescent compound (Lichtman and Conchello, 2005) and the electronic conjugation within the aromatic system is extended over the larger-size molecules. Since the overall fluorescence of WEOM extracts increased due to heating at 300 °C, this increase seems to be essentially contributed by component 1 over 2, 3 or 4, i.e., by a component of a presumably smaller size. Thus, it appears that heating the soils at 300 °C led to the preferential release of water-extractable fluorescent compounds with lower molecular weight where larger and more conjugated compounds, those ubiquitous in soils resulting from the decomposition of plant litter (Hunt and Ohno, 2007; Sharma et al., 2017a), may undergo further thermal decomposition. Remarkably, the transformations occur at temperatures of 300 °C or lower, and they are maintained at higher heating temperatures irrespective of the reduction of the amounts of TOC at 600 °C.

Changes in WEOM composition due to soil heating were also evidenced by examining ratios of NMF scores of components extracted from FTIR spectra. The scores ratio is proportional to the ratio of concentrations of those components in a soil extract. Hence, the score ratio changes may be examined quantitatively among soils or treatments, thus pointing to the changes in the ratio of component's concentrations. The NMF decomposition of FTIR spectra showed that heating resulted in an enrichment in more oxidized components in all extracts, irrespective of soil origin and properties, as reflected by the increase of the scores of component 1, which is dominated by the presence of C—O peaks, compared to the scores of other components. However, the changes in the proportion of components were only noticeable at the highest temperature. Other authors (Thurman et al., 2020; Ferrer et al., 2021) observed that heating resulted in an increase in small polycarboxylic compounds, like BPCAs (benzene polycarboxylic acids) and PCAs (pyridine carboxylic acids), and polyphenols in WEOM at temperatures higher than 250 °C. Also, Yan et al. (2022) found that the production of biochar at a temperature of 300 °C resulted in a WEOM enriched in carbohydrates. These observations could be in agreement with the findings in the present study, since fluorescence analysis indicates that soil heating contributes to WEOM with relatively smaller aromatic molecules, and FTIR shows an enrichment in a component whose most significant IR bands are commonly assigned to C—O groups. However, further research in this direction should be conducted to elaborate this analysis.

5.3. Advantages of combining fluorescence-PARAFAC and FTIR-NMF

The decomposition of spectral signatures in components with positive loadings allows an easier interpretration of the processes taking place in WEOM with soil heating. This is an advantage compared to other dimensionality reduction techniques used in soil spectroscopy, like principal component analysis or partial least squares, which yield loadings that can have positive and negative values and thus their interpretation is not straightforward. In addition, the use of the ratios of components scores obtained from dimensionality reduction techniques allows an easier quantitative evaluation of changes in WEOM composition compared to the use of intensities of absorption bands associated with certain chemical functionalities (Borisover et al., 2009, Borisover et al., 2011). This is because (i) the latter approach requires dealing with the difficult issue of separating the overlapping contributions from different functional groups, and (ii) the same chemical functionality may correspond to different WEOM components. It must be noted that components extracted from the spectral signatures are not considered to represent necessarily individual WEOM constituents. Most probably, these components represent certain conglomerates of various substances, such that the composition of these conglomerates is approximately stable among the soils and treatments studied.

We have examined the correlations between PARAFAC-based score ratios of all the fluorescent components and NMF score ratios of the components extracted from FTIR spectra. In those few cases when correlations were statistically significant, correlation coefficients did not exceed 0.35, thus suggesting that both spectroscopic techniques coupled with proper multivariate analyses provide complementary information of different aspects of WEOM compositional changes caused by soil heating. Since the cost of these spectral determinations is low, their combination could be a feasible approach for quantifying changes in WEOM composition in those studies that require to analyse a large number of samples.

6. Conclusions

In this work, the quantities and composition of WEOM from contrasting soils undergoing heating in air at two temperatures were examined. Soil heating led to significant changes in WEOM, expressed in TOC concentration, specific UV absorbance, composition of fluorescent OM, and the contribution of fluorescent OM to the whole WEOM.

PARAFAC-analyzed EEMs of fluorescence and mid-IR spectra coupled with NMF allowed to identify WEOM transformation patterns that were common to all soils, irrespective of their initial properties or origin, and each spectral technique revealed different processes. Based on fluorescence properties, the WEOM transformations caused by soil heating are understood to involve the depletion of more conjugated, bigger, fluorescent components and an enrichment in smaller, blue-shifted ones. These changes were produced at heating temperatures equal or lower than 300 °C, and sustained at temperatures as high as 600 °C. Mid-IR spectra decomposed using NMF suggested an increase of the proportion of components with more C—O bonds, more oxidized. No correlations were found between the compositional WEOM characteristics determined using fluorescence EEMs and mid-IR spectra thus indicating that the information obtained from these methods is complementary.

From the results of the present work, it can be concluded that the combination of different spectroscopic techniques coupled with dimensionality reduction methods can be used as a low cost and simple method to fingerprint changes in WEOM composition caused by fire, contributing to a better understanding of the translocations, fate, and potential risks of this highly environmentally active fraction of organic carbon by allowing the analysis of a large number of samples at low cost. Future would involve the characterization of WEOM extracts using techniques such as GC–MS or ^{13}C NMR, in order to link the changes in the spectroscopic signatures of WEOM caused by heating with detailed molecular characterizations.

Declaration of Competing Interest

The authors declare that they have no known competing financial interests or personal relationships that could have appeared to influence the work reported in this paper.

Data availability

The authors are unable or have chosen not to specify which data has been used.

References

Abdulla, H.A.N., Minor, E.C., Dias, R.F., Hatcher, P.G., 2010. Changes in the compound classes of dissolved organic matter along an estuarine transect: A study using FTIR and 13C NMR. Geochim. Cosmochim. Acta 74, 3815–3838.

Afseth, N.K., Kohler, A., 2012. Extended multiplicative signal correction in vibrational spectroscopy, a tutorial. Chemom. Intel. Lab. Syst. 117, 92–99.

Alexis, M.A., Rumpel, C., Knicker, H., Leifeld, J., Rasse, D., Péchot, N., Bardoux, G., Mariotti, A., 2010. Thermal alteration of organic matter during a shrubland fire: A field study. Organic Geochem. 41, 690–697.

Almendros, G., González-Vila, F.J., 2012. Wildfires, soil carbon balance and resilient organic matter in Mediterranean ecosystems: A review. Spanish J. Soil Sci. 2, 8–33.

Ang, A.M.S., Gillis, N., 2019. Algorithms and comparisons of nonnegative matrix factorizations with volume regularization for hyperspectral unmixing. IEEE J. Sel. Top. Appl. Earth Obs. Remote Sens. 12, 4843–4853.

Artz, R.R.E., Chapman, S.J., Jean Robertson, A.H., Potts, J.M., Laggoun-Défarge, F., Gogo, S., Comont, L., Disnar, J., Francez, A., 2008. FTIR spectroscopy can be used as a screening tool for organic matter quality in regenerating cutover peatlands. Soil Biol. Biochem. 40, 515–527.

Baghoth, S.A., Sharma, S.K., Amy, G.L., 2011. Tracking natural organic matter (NOM) in a drinking water treatment plant using fluorescence excitation–emission matrices and PARAFAC. Water Res. 45, 797–809.

Borisover, M., Laor, Y., Parparov, A., Bukhanovsky, N., Lado, M., 2009. Spatial and seasonal patterns of fluorescent organic matter in Lake Kinneret (Sea of Galilee) and its catchment basin. Water Res. 43, 3104–3116.

Borisover, M., Laor, Y., Saadi, I., Lado, M., Bukhanovsky, N., 2011. Tracing organic footprints from industrial effluent discharge in recalcitrant riverine chromophoric dissolved organic matter. Water Air Soil Pollut. 222, 255–269.

Borisover, M., Lordian, A., Levy, G.J., 2012. Water-extractable soil organic matter characterization by chromophoric indicators: Effects of soil type and irrigation water quality. Geoderma 179–180, 28–37.

Bro, R., 1997. PARAFAC. Tutorial and applications. Chemom. Intel. Lab. Syst. 38, 149–171.

Bro, R., Kjeldahl, K., Smilde, A.K., Kiers, H.A.L., 2008. Cross-validation of component models: A critical look at current methods. Anal. Bioanal. Chem. 390, 1241–1251.

Brunet, J.P., Tamayo, P., Golub, T.R., Mesirov, J.P., 2004. Metagenes and molecular pattern discovery using matrix factorization. Proc. Natl. Acad. Sci. - PNAS 101, 4164–4169.

Cauwet, G., 2002. DOM in the coastal zone. In: Hansell, D.A., Carlson, C.A. (Eds.), Biogeochemistry of Marine Dissolved Organic Matter. Academic Press, San Diego, pp. 579–609.

Cawley, K.M., Hohner, A.K., Podgorski, D.C., Cooper, W.T., Korak, J.A., Rosario-Ortiz, F. K., 2016. Molecular and spectroscopic characterization of water extractable organic matter from thermally altered soils reveal insight into disinfection byproduct precursors. Environ. Sci. Tech. 51, 771–779. https://doi.org/10.1021/acs.est.6b05126.

Certini, G., 2005. Effects of fire on properties of forest soils: a review. Oecologia 143, 1–10.

Chantigny, M.H., 2003. Dissolved and water-extractable organic matter in soils: a review on the influence of land use and management practices. Geoderma 113, 357–380.

Cheshire, M., Dumat, C., Fraser, A.R., Hillier, S., Staunton, S., 2008. The interaction between soil organic matter and soil clay minerals by selective removal and controlled addition of organic matter. Eur. J. Soil Sci. 51, 497–509.

Cory, R.M., McKnight, D.M., 2005. Fluorescence spectroscopy reveals ubiquitous presence of oxidized and reduced quinones in dissolved organic matter. Environ. Sci. Tech. 39, 8142–8149.

de Juan, A., Tauler, R., 2021. Multivariate Curve Resolution: 50 years addressing the mixture analysis problem – A review. Anal. Chim. Acta 1145, 59–78.

Dittmar, T., Paeng, J., 2009. A heat-induced molecular signature in marine dissolved organic matter. Nat. Geosci. 2, 175–179.

Dittmar, T., de Rezende, C.E., Manecki, M., Niggemann, J., Coelho Ovalle, A.R., Stubbins, A., Bernardes, M.C., 2012. Continuous flux of dissolved black carbon from a vanished tropical forest biome. Nat. Geosci. 5, 618–622.

Doerr, S., Santin, C., 2016. Global trends in wildfire and its impacts: perceptions versus realities in a changing world. Philos. Trans. R. Soc. B 371, 20150345.

Ernakovich, J.G., Wallenstein, M.D., Calderón, F.J., 2015. Chemical indicators of cryoturbation and microbial processing throughout an Alaskan permafrost soil depth profile. Soil Sci. Soc. Am. J. 79, 783–793.

Fellman, J.B., Miller, M.P., Cory, R.M., D'Amore, D.V., White, D., 2009. Characterizing dissolved organic matter using PARAFAC modeling of fluorescence spectroscopy: A comparison of two models. Environ. Sci. Technol. 43, 6228–6234.

Fernández, I., Cabaneiro, A., Carballas, T., 1997. Organic matter changes immediately after a wildfire in an Atlantic forest soil and comparison with laboratory soil heating. Soil Biol. Biochem. 29 (1), 1–11.

Ferrer, I., Thurman, E.M., Zweigenbaum, J.A., Murphy, S.F., Webster, J.P., Rosario-Ortiz, F.L., 2021. Wildfires: Identification of a new suite of aromatic polycarboxylic acids in ash and surface water. Sci. Total Environ. 770, 144661.

Fritzsche, A., Ritschel, T., Schneider, L., Totsche, K.U., 2019. Identification and quantification of single constituents in groundwater with Fourier-transform infrared spectroscopy and Positive Matrix Factorization. Vib. Spectrosc. 100, 152–158.

Fu, X., Huang, K.J., Sidiropoulos, N.D., 2018. On Identifiability of Nonnegative Matrix Factorization. IEEE Signal Process Lett. 25, 328–332.

Fu, X., Huang, K., Sidiropoulos, N.D., Shi, Q., Hong, M., 2019. Anchor-Free correlated topic modeling. TPAMI 41, 1056–1071.

Gee, G.W. and Or, D., 2002. 2.4 Particle-Size Analysis. Methods of Soil Analysis, :255-293.

Giglio, L., Randerson, J.T., van der Werf, G.R., 2013. Analysis of daily, monthly, and annual burned area using the fourth-generation global fire emissions database (GFED4). J. Geophys. Res. Biogeo. 118, 317–328.

González-Pérez, J.A., González-Vila, F.J., Almendros, G., Knicker, H., 2004. The effect of fire on soil organic matter-a review. Environ. Int. 30 (6), 855–870.

Grandy, A.S., Neff, J.C., 2008. Molecular C dynamics downstream: The biochemical decomposition sequence and its impact on soil organic matter structure and function. Sci. Total Environ. 404, 297–307.

Gu, W., Huang, S., Lei, S., Yue, J., Su, Z., Si, F., 2019. Quantity and quality variations of dissolved organic matter (DOM) in column leaching process from agricultural soil: Hydrochemical effects and DOM fractionation. Sci. Total Environ. 691, 407–416.

Gu, B., Schmitt, J., Chen, Z., Liang, L., McCarthy, J.F., 1995. Adsorption and desorption of different organic matter fractions on iron oxide. Geochim. Cosmochim. Acta 59, 219–229.

Guo, M., Chorover, J., 2003. Transport and fractionation of dissolved organic matter in soil columns. Soil Sci. 168.

Hadas, A., Kautsky, L., Goek, M., Kara, E.E., 2004. Rates of decomposition of lant residues and available nitrogen in soil, related to residue composition through simulation of carbon and nitrogen turnover. Soil Biol. Biochem. 36, 255–266.

Helwig, N.E., 2019. multiway: Component models for multi-way data. Package version 1.0-6. URL: https://CRAN.R-project.org/package=multiway.

Henry, E.R., Hofrichter, J., 1992. Singular value decomposition : application to analysis of experimental data. Methods Enzymol. 210, 129–192.

Hobley, E.U., Zoor, L.C., Shrestha, H.R., Bennett, L.T., Weston, C.J., Baker, T.G., 2019. Prescribed fire affects the concentration and aromaticity of soluble soil organic matter in forest soils. Geoderma 341, 138–147.

Holbrook, R.D., DeRose, P.C., Leigh, S.D., Rukhin, A.L., Heckert, N.A., 2006. Excitation-Emission matrix fluorescence spectroscopy for natural organic matter characterization: a quantitative evaluation of calibration and spectral correction procedures. Appl. Spectrosc. 60 (7), 791–799.

Hu, B., Wang, P., Wang, C., Qian, J., Bao, T., Shi, Y., 2019. Investigating spectroscopic and copper-binding characteristics of organic matter derived from sediments and suspended particles using EEM-PARAFAC combined with two-dimensional fluorescence/FTIR correlation analyses. Chemosphere 219, 45–53.

Hunt, J.F., Ohno, T., 2007. Characterization of fresh and decomposed dissolved organic matter using excitation−emission matrix fluorescence spectroscopy and multiway analysis. J. Agric. Food Chem. 55, 2121–2128.

Ilani, T., Schulz, E., Chefetz, B., 2005. Interactions of organic compounds with wastewater dissolved organic matter: role of hydrophobic fractions. J. Environ. Qual. 34, 552–562.

Ishii, S.K.L., Boyer, T.H., 2012. Behavior of feoccurring PARAFAC components in fluorescent dissolved organic matter in natural and engineered systems: A critical review. Environ. Sci. Tech. 46, 2006–2017.

IUSS Working Group WRB. 2015. World Reference Base for Soil Resources 2014, update 2015 International soil classification system for naming soils and creating legends for soil maps. World Soil Resources Reports No. 106. FAO, Rome.

Jones, M.W., Coppola, A.I., Santín, C., Dittmar, T., Jaffé, R., Doerr, S.H., Quine, T.A., 2020. Fires prime terrestrial organic carbon for riverine export to the global oceans. Nat. Commun. 11, 2791.

Kaiser, K., Guggenberger, G., Haumaier, L., Zech, W., 1997. Dissolved organic matter sorption on sub soils and minerals studied by 13C-NMR and DRIFT spectroscopy. Eur. J. Soil Sci. 48, 301–310.

Kalakodio, L., Alepu, O.E., Zewde, A.A., 2017. Application of techniques derived from the study of soil organic matter to characterize the organic matter during the composting of various materials-A review. J. Pollut. Effects Control 5.

Kalbitz, K., Solinger, S., Park, J., Michalzik, B., Matzner, E., 2000. Controls on the dynamics of dissolved organic matter in soils: A review. Soil Sci. 165.

Knicker, H., 2007. How does fire affect the nature and stability of soil organic nitrogen and carbon? A review. Biogeochemistry 85, 91–118.

Kothawala, D.N., Murphy, K.R., Stedmon, C.A., Weyhenmeyer, G.A., Tranvik, L.J., 2013. Inner filter correction of dissolved organic matter fluorescence. Limnol. Oceanogr. Methods 11, 616–630.

Lakowicz, J.R., 2013. Principles of Fluorescence Spectroscopy. Springer Science & Business Media.

Lambert, T., Bouillon, S., Darchambeau, F., Massicotte, P., Borges, A.V., 2016. Shift in the chemical composition of dissolved organic matter in the Congo River network. Biogeosciences 13, 5405–5420.

Lee, D.D., Seung, H.S., 1999. Learning the parts of objects by non-negative matrix factorization. Nature 401, 788–791.

Li, X., Dai, X., Dai, L., Liu, Z., 2015. Two-dimensional FTIR correlation spectroscopy reveals chemical changes in dissolved organic matter during the biodrying process of raw sludge and anaerobically digested sludge. RSC Adv. 5, 82087–82096.
Lichtman, J.W., Conchello, J.A., 2005. Fluorescence microscopy. Nat. Methods 2 (13), 910–919. https://doi.org/10.1038/NMETH817.
Liland, K.H., 2021. EMSC: Extended Multiplicative Signal Correction. R package version (9), 3.
Loeppert, R.H., and Suarez, D.L., 1996. Carbonate and gypsum. in: Sparks, D.L., et al., Eds., Methods of Soil Analysis. Part 3. Chemical Methods, ASA and SSSA, Madison, 437-474. doi:10.2136/sssabookser5.3.c15.
Matamala, R., Calderón, F.J., Jastrow, J.D., Fan, Z., Hofmann, S.M., Michaelson, G.J., Mishra, U., Ping, C., 2017. Influence of site and soil properties on the DRIFT spectra of northern cold-region soils. Geoderma 305, 80–91.
McKay, G., Hohner, A., Rosario-Ortiz, F.L., 2020. Use of optical properties for evaluating the presence of pyrogenic organic matter in thermally altered soil leachates. Environ. Sci. Processes Impacts 22, 981. https://doi.org/10.1039/c9em00413k.
Miesel, J.R., Hockaday, W.C., Kolka, R.K., Townsend, P.A., 2015. Soil organic matter composition and quality across fire severity gradients in coniferous and deciduous forests of the southern boreal region. J. Geophys. Res. Biogeo. 120, 1124–1141.
Mitchell, P.J., Simpson, A.J., Soong, R., Simpson, M.J., 2015. Shifts in microbial community and water-extractable organic matter composition with biochar amendment in a temperate forest soil. Soil Biol. Biochem. 81, 244–254. https://doi.org/10.1016/j.soilbio.2014.11.017.
Montcuquet, A., Hervé, L., Navarro, F., Dinten, J., Mars, J.I., 2010. Nonnegative matrix factorization: a blind spectra separation method for in vivo fluorescent optical imaging. J. Biomed. Opt. 15, 056009.
Murphy, K.R., Stedmon, C.A., Waite, T.D., Ruiz, G.M., 2008. Distinguishing between terrestrial and autochthonous organic matter sources in marine environments using fluorescence spectroscopy. Mar. Chem. 108, 40–58.
Näthe, K., Levia, D.F., Steffens, M., Michalzik, B., 2017. Solid-state 13C NMR characterization of surface fire effects on the composition of organic matter in both soil and soil solution from a coniferous forest. Geoderma 305, 394–406.
Nelson, D.W., Sommers, L.E., 1996. Total Carbon, Organic Carbon, and Organic Matter. Methods Soil Anal. 961–1010.
Niemeyer, J., Chen, Y., Bollag, J.M., 1992. Characterization of humic acids, composts, and peat by diffuse reflectance Fourier-transform infrared spectroscopy. Soil Sci. Soc. Am. J. 56, 135–140.
Ohno, T., Bro, R., 2006. Dissolved organic matter characterization using multiway spectral decomposition of fluorescence landscapes. Soil Sci. Soc. Am. J. 70, 2028–2037.
Oren, A., Chefetz, B., 2012. Sorptive and desorptive fractionation of dissolved organic matter by mineral soil matrices. J. Environ. Qual. 41, 526–533.
Parikh, S.J., Goyne, K.W., Margenot, A.J., Mukome, F.N.D., Calderón, F.J., 2014. Soil chemical insights provided through vibrational spectroscopy. Adv. Agron. 126, 1–148.
Peltre, C., Bruun, S., Du, C., Thomsen, I.K., Jensen, L.S., 2014. Assessing soil constituents and labile soil organic carbon by mid-infrared photoacoustic spectroscopy. Soil Biol. Biochem. 77, 41–50.
Podgorski, D.C., Zito, P., McGuire, J.T., Martinovic-Weigelt, D., Cozzarelli, I.M., Bekins, B.A., Spencer, R.G.M., 2018. Examining natural attenuation and acute toxicity of petroleum-derived dissolved organic matter with optical spectroscopy. Environ. Sci. Tech. 52, 6157–6166.
Prokop, Z., Cupr, P., Zlevorova-Zlamalikova, V., Komarek, J., Dusek, L., Holoubek, I., 2003. Mobility, bioavailability, and toxic effects of cadmium in soil samples. Environ. Res. 91, 119–126.
R Core Team, 2021. R: A language and environment for statistical computing. R Foundation for Statistical Computing, Vienna, Austria. URL https://www.R-project.org/.
Rees, R.M., Parker, J.P., 2005. Filtration increases the correlation between water extractable organic carbon and soil microbial activity. Soil Biol. Biochem. 37, 2240–2248.
Rein, G., Cleaver, N., Ashton, C., Pironi, P., Torero, J.L., 2008. The severity of smouldering peat fires and damage to the forest soil. Catena 74, 304–309.
Revchuk, A.D., Suffet, I.H., 2014. Effect of wildfires on physicochemical changes of watershed dissolved organic matter. Water Environ. Res. 86, 372–381.
Rhymes, J.M., Cordero, I., Chomel, M., Lavallee, J.M., Straathof, A.K., Ashworth, D., Langridge, H., Semchenko, M., de Vries, F.T., Johnson, D., Bardgett, R.D., 2021. Are researchers following best storage practices for measuring soil biochemical properties. Soil 7, 95–106.
Ritschel, T., Totsche, K.U., 2017. Quantification of pH-dependent speciation of organic compounds with spectroscopy and chemometrics. Chemosphere 172, 175–184.
Roth, V., Dittmar, T., Gaupp, R., Gleixner, G., 2014. Ecosystem-specific composition of dissolved organic matter. Vadose Zone J. 13.
Santos, F., Russel, D., Berhe, A.A., 2016. Thermal alteration of water extractable organic matter in climosequence soils from the Sierra Nevada, California. J. Geophys. Res. Biogeosci. 121, 2877–2885. https://doi.org/10.1002/2016JG003597.
Sauwen, N., Acou, M., Bharath, H.N., Sima, D.M., Veraart, J., Maes, F., Himmelreich, U., Achten, E., Van Huffel, S., 2017. The successive projection algorithm as an initialization method for brain tumor segmentation using non-negative matrix factorization. PLoS One 12, e0180268.
Sharma, P., Laor, Y., Raviv, M., Medina, S., Saadi, I., Krasnovsky, A., Vager, M., Levy, G. J., Bar-Tal, A., Borisover, M., 2017a. Compositional characteristics of organic matter and its water-extractable components across a profile of organically managed soil. Geoderma 286, 73–82.
Sharma, P., Laor, Y., Raviv, M., Medina, S., Saadi, I., Krasnovsky, A., Vager, M., Levy, G. J., Bar-Tal, A., Borisover, M., 2017b. Green manure as part of organic management cycle: Effects on changes in organic matter characteristics across the soil profile. Geoderma 305, 197–207.
Silverstein, R.M., Kiemle, D.J., Bryce, D.L., Webster, F.X., 2015. Spectrometric Identification of Organic Compounds. Wiley.
Soldatov, R., Kharchenko, P., Biederstedt, E., 2021. vrnmf: Volume-regularized structured matrix factorization. R package version 1.
Spark, K., Swift, R., 2002. Effect of soil composition and dissolved organic matter on pesticide sorption. Sci. Total Environ. 298, 147–161.
Steel, R.G.D., Torrie, J.H., 1960. Principles and Procedures of Statistics. McGraw-Hill Book Company Inc, New York, Toronto, London.
Stirling, E., Macdonald, L.M., Smernik, R.J., Cavagnaro, T.R., 2019. Post fire litters are richer in water soluble carbon and lead to increased microbial activity. Appl. Soil Ecol. 136, 101–105.
Sumner, M.E. and Miller, W.P., 1996. Cation Exchange Capacity and Exchange Coefficients. Methods of Soil Analysis, :1201-1229.
Sun, K., Jin, J., Kang, M., Zhang, Z., Pan, Z., Wang, Z., Wu, F., Xing, B., 2013. Isolation and characterization of different organic matter fractions from a same soil source and their phenanthrene sorption. Environ. Sci. Tech. 47, 5138–5145.
Thurman, E.M., Yu, Y., Ferrer, I., Thorn, K.A., Rosario-Ortiz, F.L., 2020. Molecular identification of water-extractable organic carbon from thermally heated soils: C–13 NMR and accurate mass analyses find benzene and pyridine carboxylic acids. Environ. Sci. Tech. 54, 2994–3001.
Traoré, M., Kaal, J., Martínez Cortizas, A., 2016. Application of FTIR spectroscopy to the characterization of archeological wood. Spectrochim. Acta Part A, Mol. Biomol. Spectrosc. 153, 63–70.
Trompowsky, P.M., Benites, V.D.M., Madari, B.E., Pimenta, A.S., Hockaday, W.C., Hatcher, P.G., 2005. Characterization of humic like substances obtained by chemical oxidation of eucalyptus charcoal. Org. Geochem. 36, 1480–1489.
Vazquez-Ortega, A., Hernandez-Ruiz, S., Amistadi, M.K., Rasmussen, C., Chorover, J., 2014. Fractionation of dissolved organic matter by (Oxy)Hydroxide-coated sands: competitive sorbate displacement during reactive transport. Vadose Zone J. 13.
Vergnoux, A., Di Rocco, R., Domeizel, M., Guiliano, M., Doumenq, P., Théraulaz, F., 2011. Effects of forest fires on water extractable organic matter and humic substances from Mediterranean soils: UV–vis and fluorescence spectroscopy approaches. Geoderma 160, 434–443.
Wang, G., Ding, Q., Hou, Z., 2008. Independent component analysis and its applications in signal processing for analytical chemistry. Trac-Trends Anal. Chem. 27, 368–376.
Weishaar, J.L., Aiken, G.R., Bergamaschi, B.A., Fram, M.S., Fujii, R., Mopper, K., 2003. Evaluation of specific ultraviolet absorbance as an indicator of the chemical composition and reactivity of dissolved organic carbon. Environ. Sci. Tech. 37 (20), 4702–4708.
Yan, W., Chen, Y., Han, L., Sun, K., Song, F., Yang, Y., Sun, H., 2022. Pyrogenic dissolved organic matter produced at higher temperature is more photoactive: Insight into molecular changes and reactive oxygen species generation. J. Hazard. Mater. 425, 127817.
Yan, J., Manelski, R., Vasilas, B., Jin, Y., 2018. Mobile colloidal organic carbon: An underestimated carbonn pool in global carbon cycles? Front. Environ. Sci. 6, 148. https://doi.org/10.3389/fenvs.2018.00148.
Yang, H., Seoighe, C., 2016. Impact of the choice of normalization method on molecular cancer class discovery using nonnegative matrix factorization. PLoS One 11, e0164880.
Zhang, Y., Wang, X., Wang, X., Li, M., 2019. Effects of land use on characteristics of water-extracted organic matter in soils of arid and semi-arid regions. Environ. Sci. Pollut. Res. 26, 26052–26059.